Optimal Design of Hybrid Energy System with PV/ Wind Turbine/ Storage: A Case Study

Rui Huang, Steven H. Low, Ufuk Topcu, K. Mani Chandy
Computing Mathematical Sciences, California Institute of Technology, USA
Christopher R. Clarke
Southern California Edison, USA

***Abstract*—Hybrid energy systems with renewable generation are built in many remote areas where the renewable resources are abundant and the environment is clean. We present a case study of the Catalina Island in California for which a system with photovoltaic (PV) arrays, wind turbines, and battery storage is designed based on empirical weather and load data. To determine the system size, we formulate an optimization problem that minimizes the total construction and operation cost subject to maximum tolerable risk. Simulations using the Hybrid Optimization Model for Electric Renewable (HOMER) is used to determine the feasible set of the optimization problem.**

I. Introduction

Power networks at remote areas that use conventional energy sources such as diesel often face particularly high fuel transportation and environmental costs [1], [2]. With the rapid development of photovoltaic (PV), wind turbine and battery technologies, hybrid energy system has received increasing attention as an alternative to conventional system, with diesel generation only as emergency backup [3]. The Santa Catalina Island is 26 miles off the coast of Long Beach and belongs to the Los Angeles County in California. It is 21 miles long, 76 square miles in area, with 54 miles of coastline. It is served by three 12 kV distribution circuits that are separate from the grid on the mainland. Electricity is currently generated by diesel, which is transported by ship from the mainland. The peak demand in 2008 was around 5.3 MW. In this paper, we investigate the feasibility of replacing the diesel generation with renewable resources such as solar and wind power, supplemented with battery storage in a case study.

One of the key impediments of such a hybrid system is the intermittency and uncertainty of the renewable outputs. We adopt a risk-limiting approach in our design [4]. Specifically, we consider a hypothetical scenario where the island is completely powered by renewable sources and calculate the system size – the size of PV arrays, the number of wind turbines and the capacity of battery storage – that limit the risk that the supply is insufficient to balance the demand to an acceptable risk level. We then choose a minimum-cost design among all the designs that have the same risk.

In Section II, we describe a simple model for our hybrid energy system and the representative weather and load data that form the basis of the design. A Markov chain approximation of this model is used in [8] to calculate numerically the set of admissible designs that achieve a given risk tolerance. Here, we use the empirical data to drive the simulator Hybrid Optimization for Electric Renewable (HOMER) developed by National Renewable Energy Laboratory (NREL) [5] to simulate the admissible designs. More detailed comparison between these two approaches is given in Section III. In Section IV, we formulate an optimal design problem using a cost function from the literature and a feasible set from the HOMER simulations. We illustrate a risk-limiting approach that minimizes the total construction and operation cost with an example design.

Our case study represents a back-of-the-envelop estimate of a feasible design. The simple model we use does not take into account the power flow constraints on the distribution circuits, effectively assuming that the network is not a bottleneck. It also does not consider transient stability in the presence of large, rapid, and random fluctuations of renewable outputs.

II. A simple system model

In this section, we first describe a simple model of the hybrid energy system that consists of PV arrays, wind turbines and battery storage and use that to define the set of *admissible designs* as our design space. Then we describe empirical data we will use to compute admissible designs using the HOMER simulator. The simulations are detailed in the next section.

A. A model of load-shedding

We consider the system configuration in Figure 1 for the Catalina Island. Here, $d(t)$, $b(t)$, $s(t)$ and $w(t)$ denote respectively the amount of demand, the amount of energy stored in the battery, the amount of energy generated by each PV array of 1 kW capacity, and the amount of energy generated by each 1 kW wind turbine at time t. For a system with γ_1 number of

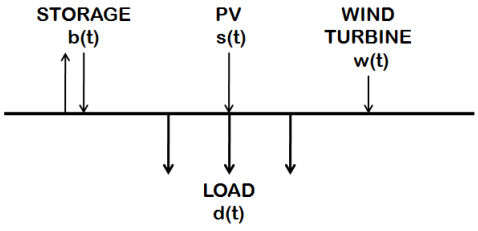

Fig. 1. The hybrid energy system with PV/ wind turbine/ battery storage for the Catalina Island.

PV arrays and γ_2 number of wind turbines, the total generation by renewable resources is:

$$g(t) \quad := \quad \gamma_1 s(t) + \gamma_2 w(t). \tag{1}$$

Clearly $g(t)$ is upper bounded by $\gamma_1 + \gamma_2$ kW. We assume the battery has an energy capacity of $\overline{b} \geq 0$ and a minimum state of charge of $\underline{b} \geq 0$. We use a simple deterministic battery

978-1-4577-1702-4/11/$26.00 ©2011 IEEE

model where the state of charge $b(t)$ is given by a recursion of the form:

$$b(t+1) \quad = \quad b(t) + f\left(b(t), g(t) - d(t); \underline{b}, \bar{b}\right), \qquad (2)$$

i.e., the state of charge $b(t+1)$ in the next period depends on the current state of charge $b(t)$ and the net generation $g(t) - d(t)$. When $g(t) > d(t)$, $g(t) - d(t)$ is the excess generation, the battery will be charged, and $f(b(t), g(t) - d(t); \underline{b}, \bar{b}) \geq 0$. When $g(t) < d(t)$, $g(t) - d(t)$ is the generation shortfall, the battery will discharge, and $f(b(t), g(t) - d(t); \underline{b}, \bar{b}) \leq 0$.

For instance, the HOMER simulations described in Section III can be modeled by the following:

$$b(t+1) \quad = \quad b(t) + [g(t) - d(t)]_{-r_2(t)}^{r_1(t)}, \qquad (3)$$

where $[x]_a^c = \max\{\min\{x, c\}, a\}$, $a < c$, and

$$r_1(t) \quad := \quad \alpha_1(\bar{b} - b(t)), \qquad (4)$$

$$r_2(t) \quad := \quad \alpha_2(b(t) - \underline{b}), \qquad (5)$$

where $\alpha_1, \alpha_2 \in (0, 1)$. This means that the time-dependent maximum charging rate (per time period) is $r_1(t)$ and the time-dependent maximum discharging rate is $r_2(t)$. Moreover, $r_1(t)$ ($r_2(t)$) is a fraction α_1 (α_2) of the gap between the current state of charge $b(t)$ and the capacity $\bar{b}$ (the minimum state of charge $\underline{b}$). Note that if $b(0) \in [\underline{b}, \bar{b}]$, then $b(t) \in [\underline{b}, \bar{b}]$ for all $t \geq 1$. If the battery has a charging efficiency of $\epsilon_1 \in (0, 1]$ and a discharging efficiency of $\epsilon_2 \in (0, 1]$, this can be modeled by replacing the function f in (3) by

$$f \quad = \quad \begin{cases} \min\{\epsilon_1(g(t) - d(t)), r_1(t)\}, & \text{if } g(t) \geq d(t). \\ \max\{\epsilon_2^{-1}(g(t) - d(t)), -r_2(t)\}, & \text{otherwise.} \end{cases} \qquad (6)$$

An important consideration of the reliability of any power system is whether the demand can be met, and when the demand is not met, what is the extent of the shortage. When demand $d(t)$ exceeds the sum of the generation $g(t)$ and the energy that can be supplied by the battery, we say that *a load-shedding event* has occurred. For the model given by (2)–(6), a load-shedding event has occurred if

$$\epsilon_2^{-1}(d(t) - g(t)) \quad > \quad r_2(t) := \alpha_2(b(t) - \underline{b}), \qquad (7)$$

i.e., when the amount of energy that must be drawn from the battery to cover the generation shortfall exceeds the maximum discharge rate $r_2(t)$ which is smaller than the state of charge $b(t)$.

We measure risk by two quantities: F_t is the fraction of time when a load-shedding event occurs over the horizon $[1, T]$, e.g., over one year, so $T = 8760$ hours and F_e is the fraction of energy not served when a load-shedding event occurs over the horizon $[1, T]$. Formally, let the times when a load-shedding event occurs be denoted by

$$L \quad := \quad \{\ t \mid (7) \text{ holds } \}. \qquad (8)$$

Then

$$F_t \quad := \quad \frac{|L|}{T}. \qquad (9)$$

When a load-shedding event occurs at time t, the amount of excess demand that is filled by the energy stored in the battery is given by $\epsilon_2 r_2(t) = \epsilon_2\alpha_2(b(t) - \underline{b})$. Hence,

$$F_e \quad := \quad \frac{\sum_{t \in L} d(t) - g(t) - \epsilon_2\alpha_2(b(t) - \underline{b})}{\sum_t d(t)}. \qquad (10)$$

Clearly F_t and F_e depends on the system sizes $(\gamma_1, \gamma_2, \bar{b})$.

In summary, our model for the energy system is specified by (1)–(6), and the risks are defined by (9)–(10). Clearly, the risks F_t and F_e depend on the system sizes $(\gamma_1, \gamma_2, \bar{b})$. We call a 3-tuple $(\gamma_1, \gamma_2, \bar{b})$ a *design*. A design $(\gamma_1, \gamma_2, \bar{b})$ is *admissible with respect to* $\epsilon \in [0, 1]$ if the resulting $F_t \leq \epsilon$, or if the resulting $F_e \leq \epsilon$. We are interested in the set of admissible designs and we will use the HOMER simulator to calculate these admissible designs. For this purpose, we now describe empirical weather and load data that will drive HOMER simulations.

B. Solar Radiation and Wind Speed Data

The HOMER simulator will be driven by traces of solar power output $s(t)$ and wind power output $w(t)$ (see (1)). These traces are obtained from empirical data on solar radiation and wind speed at locations close to the Catalina Island, as we now explain.

Hourly solar radiation data in one year are obtained from NREL, available at [6]. We use the hourly data for Long Beach, California (longitude: 33.8, latitude: -118.2) from the 1991-2005 National Solar Radiation Database. The hourly solar radiation data are plotted in Figure 2.

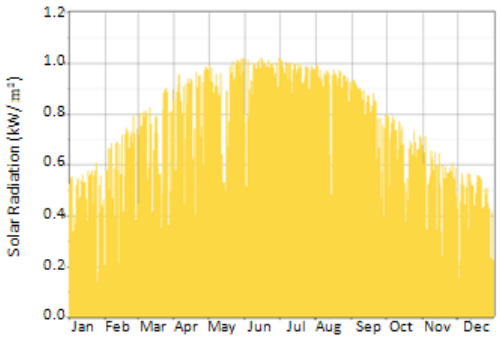

Fig. 2. Hourly solar radiation in one year on Long Beach, CA, USA.

Hourly wind speed data in one year are obtained from NREL, available at [7]. We use the hourly data for a wind plant station located on an island off the coast of Santa Barbara, California (longitude: 34.4, latitude: -119.7). The hourly wind speed data are plotted in Figure 3.

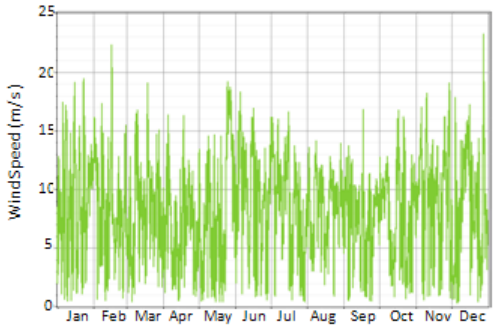

Fig. 3. Hourly wind speed in one year on an island off the coast of Santa Barbara, CA, USA.

C. Load Profile

For $d(t)$ in the model (2), we use the representative (proxy) load data are obtained from Southern California Edison (SCE) from April, 2009 to March, 2010 for Santa Catalina, California (longitude: 33.4, latitude: -118.4), and final load profile in one year is generated as explained in [8]. The hourly load data are plotted in Figure 3. The annual average load demand is 39 MWh/day. The peak demand was 5.3 MW.

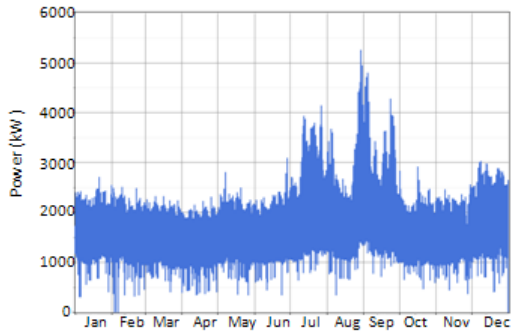

Fig. 4. Hourly load demand in one year on the Catalina Island, CA, USA.

III. Admissible Designs from HOMER Simulation

In [8], we assume a simple f (identity function) in our model (1)–(2) and approximate the process $b(t)$ as a Markov chain. We estimate the state transition probability for the Markov chain using the empirical weather and load data, and then calculate the stationary distribution of the chain. From the stationary distribution, we estimate analytically F_t and F_e and derive the admissible designs. In this paper, we adopt a different approach.

HOMER simulator has built-in modules that compute solar and wind power output from weather data. It also has built-in modules that simulate various battery dynamics. With these functions, we will use the weather and load data described in Section II and configure HOMER built-in modules to simulate the resulting system with varying choices of design parameters $(\gamma_1, \gamma_2, \bar{b})$. For each design, the simulation result yields the risks F_t or F_e. Given any acceptable risk level $\epsilon \in [0, 1]$, these simulation results therefore defines the set of admissible designs. These sets of admissible designs will be used to determine the minimum-cost design with acceptable risk in the next section. We next describe our HOMER simulations and the resulting admissible designs.

Compared with the approach in [8], the HOMER simulation captures the system dynamics more accurately than simple analytical model and therefore avoids artifacts of the analytical approximations in the model of [8]. On the other hand, in practice, both the weather and the load data are stochastic. The Markov chain model of [8] incorporates this uncertainty and estimates the admissible designs from the "average" behavior, whereas here the HOMER simulator essentially simulates only one realization of the stochastic process. We aim to compare the results of the two approches, in order to approve the accuracy of the model in [8]. But this part will be our future work which is not included here.

A. HOMER simulation

We build a hybrid energy system in HOMER with PV arrays, wind turbines and battery storage for the Catalina Island. The system configuration is shown in Figure 5. In this schematic figure, renewable energy power is generated by PV arrays and wind turbines. The generated power plus the energy stored in the battery is used to meet the load demand. Catalina Primary Load is the electrical load that the system must meet in order to avoid unmet load. A converter is used to transform the energy from DC to AC to serve the load. Input information in HOMER includes hourly solar radiation, hourly wind speed and hourly load data, as explained in Section II.

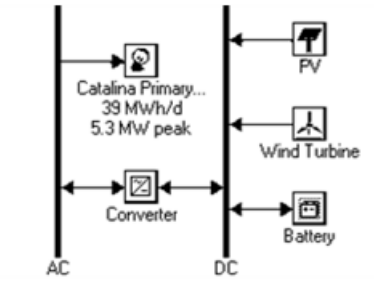

Fig. 5. The hybrid energy system with PV/ wind turbine/ battery storage for Catalina Island in HOMER.

The parameters of the system components $(\gamma_1, \gamma_2, \bar{b}$ and others) used in the HOMER simulations are shown in Table I. The time horizon T is chosen to be 8760 hours (one year).

TABLE I
Range and Type of Simulation Components.

Components	*Range*
PV Arrays	
Size	0-10,000 kW
Wind Turbine	
Number	0-10,000
Type	Generic standard 1 kW turbine
Battery	
Energy Capacity $\bar{b}$	15, 20 MWh
Minimum State of Charge $\underline{b}$	10 %
Fraction α_1	0.8
Fraction α_2	0.8
Charging Efficiency ϵ_1	90%
Discharging Efficiency ϵ_2	90%

B. Simulation Results

We conducted HOMER simulations using the solar radiation data, wind speed data, and load data. Then several simulations of different designs with different values of $(\gamma_1, \gamma_2, \bar{b})$ have been made in HOMER.

Figure 6 shows the distribution of F_t in one year as a function of γ_1 and γ_2 with battery capacity of $\bar{b} = 15$ MWh. There are at least two points that are of interest.

• As γ_1 PV arrays increases, F_t decreases. When γ_1 varies above 5000 kW, F_t varies slowly for fixed γ_2. Especially, for $F_t = 30\%$, the curve approaches a constant value when γ_1 varies above 5000 kW. We see that in Section II, the sunlight over a day is very regular and the peak demand is around 5 MW on Catalina. Therefore 5000 kW PV arrays is enough to meet the unmet load when sunlight is abundant. More than 5000 kW PV arrays will only reduce F_t to a limited extent.

• As γ_2 wind turbines increases, F_t also decreases. When γ_2 varies above 5000, F_t also varies slowly but the trend is better than γ_1. This can be attributed to the irregularity and unpredictability of wind speed, compared with solar radiation.

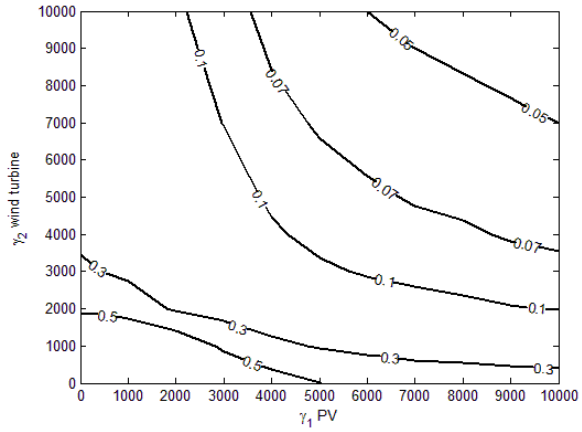

Fig. 6. The fraction of time when a load-shedding event occurs in one year as a function of γ_1 and γ_2 with battery capacity of $\bar{b} = 15$ MWh.

Figure 7 shows the distribution of F_t in one year as a function of γ_1 and γ_2 with battery capacity of $\bar{b} = 20$ MWh. There are at least two points that are of interest.

• Similar trends can be found in Figure 7. As renewable generation size increases, F_t decreases.

• For fixed F_t, the renewable generation size is smaller with $\bar{b} = 20$ MWh than that with $\bar{b} = 15$ MWh.

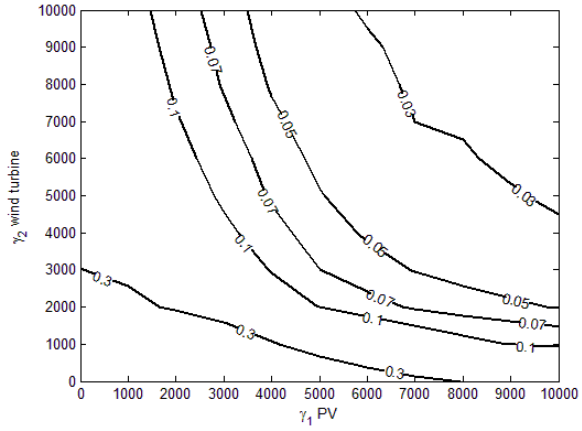

Fig. 7. The fraction of time when a load-shedding event occurs in one year as a function of γ_1 and γ_2 with battery capacity of $\bar{b} = 20$ MWh.

Figure 8 and Figure 9 respectively show the distribution of F_e in one year as a function of γ_1 and γ_2 with battery capacity of $\bar{b} = 15$ MWh and $\bar{b} = 20$ MWh. We can see similar trends as we explained in Figure 6 and Figure 7.

IV. Optimal Design

In this section, we will propose a way to choose among these multiple admissible designs, and illustrate our approach with an example.

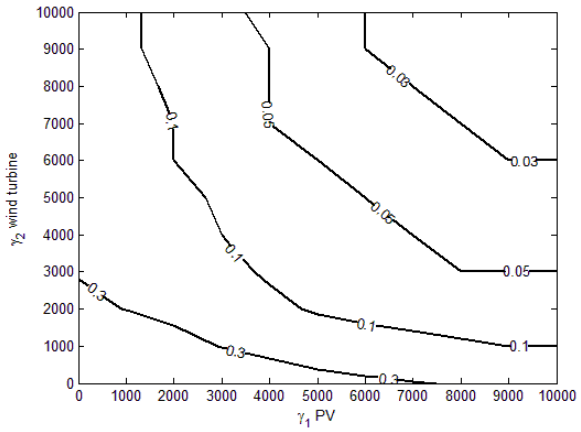

Fig. 8. The fraction of energy not served when a load-shedding event occurs in one year as a function of γ_1 and γ_2 with battery capacity of $\bar{b} = 15$ MWh.

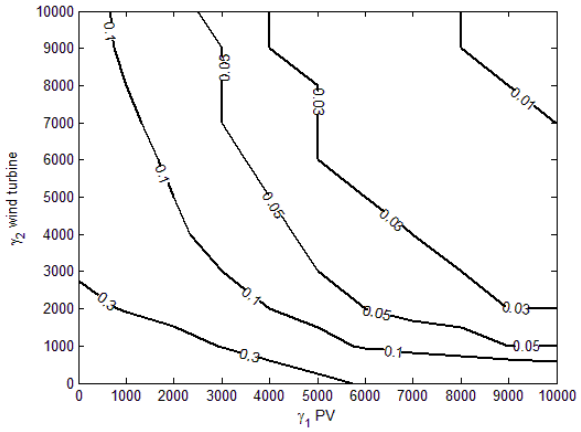

Fig. 9. The fraction of energy not served when a load-shedding event occurs in one year as a function of γ_1 and γ_2 with battery capacity of $\bar{b} = 20$ MWh.

A. Problem formulation

Note that the design process is about the tradeoff between system sizes $(\gamma_1, \gamma_2, \bar{b})$ and the acceptable risk level F_t or F_e. Therefore, we start with a specified risk level ϵ. This narrows the design choices to the admissible designs $(\gamma_1, \gamma_2, \bar{b})$ with respect to ϵ. We propose to choose a minimum-cost design among this set.

Formally, let $C(\gamma_1, \gamma_2, \bar{b})$ be a cost function that represents the total construction and operation costs operating a system of size $(\gamma_1, \gamma_2, \bar{b})$. Let $\epsilon \in [0, 1]$ be the acceptable risk level (F_t or F_e). Let the set of admissible designs with respect to ϵ be denoted by

$$X_t(\epsilon) \quad := \quad \{(\gamma_1, \gamma_2, \bar{b}) \geq 0 \mid F_t \leq \epsilon\},$$

if F_t is used as the measure of risk, and by

$$X_e(\epsilon) \quad := \quad \{(\gamma_1, \gamma_2, \bar{b}) \geq 0 \mid F_e \leq \epsilon\},$$

if F_e is used as the measure of risk. Then an *optimal design* $(\gamma_1^*, \gamma_2^*, \bar{b}^*)$ is a solution of the following constrained optimization:

$$\min_{\gamma_1, \gamma_2, \bar{b}} \quad C(\gamma_1, \gamma_2, \bar{b}) \tag{11}$$

$$\text{subject to} \quad (\gamma_1, \gamma_2, \bar{b}) \in X_t(\epsilon). \tag{12}$$

or

$$\min_{\gamma_1,\gamma_2,\bar{b}} \quad C(\gamma_1,\gamma_2,\bar{b}) \tag{13}$$

$$\text{subject to} \quad (\gamma_1,\gamma_2,\bar{b}) \in X_e(\epsilon). \tag{14}$$

depending on the desired risk measure.

In summary, our design process follows the following steps:

1) Obtain realistic solar radiation and wind speed data representative of the location of the design.
2) Obtain representative load data.
3) Specify the desired risk measure F_t or F_e and acceptable risk level ϵ.
4) Use a realistic simulator, e.g., HOMER, to characterize the feasible set $X_t(\epsilon)$ or $X_e(\epsilon)$ based on the weather and load data.
5) Determine the cost function $C(\gamma_1,\gamma_2,\bar{b})$.
6) Estimate a solution to the optimization problem (11)–(12) or (13)–(14) for an optimal design $(\gamma_1^*,\gamma_2^*,\bar{b}^*)$.

B. Case study

We first describe a cost model $C(\gamma_1,\gamma_2,\bar{b})$ from the literature and then solve for the optimal designs following the steps outlined above in this section.

1) Cost Model: We use the cost function proposed in [9] that includes the total construction and operation cost. To simplify notation, we will omit the argument and write C instead of $C(\gamma_1,\gamma_2,\bar{b})$.

The cost model in [9] breaks the total cost into costs of four system components, PV arrays, wind turbines, battery and converter:

$$C \quad = \quad C_{PV} + C_{WT} + C_{BA} + C_{CONV}. \tag{15}$$

For each system component, the cost is as follows:

$$\begin{aligned} C_{PV} &= C_{module} \times \gamma_1 + C_{O\&M1} \times \gamma_1 \times Life, \\ C_{WT} &= C_{turbine} \times \gamma_2 + C_{O\&M2} \times \gamma_2 \times Life, \\ C_{BA} &= C_{battery} \times \bar{b}, \\ C_{CONV} &= C_{converter} \times S_{CONV}. \end{aligned} \tag{16}$$

Here C_{module} is the capital cost for 1 kW module, $C_{O\&M1}$ is the operation/maintenance cost for PV arrays per kW per year. $C_{turbine}$ is the capital cost for one 1 kW wind turbine, $C_{O\&M2}$ is the operation/maintenance cost for one 1 kW wind turbine per year. $C_{battery}$ is the capital cost for 1 kWh battery. $C_{converter}$ is the capital cost for 1 kW converter, S_{CONV} is the capacity of converter. In our design, we fix the size S_{CONV} as 6 MW, which is slightly larger than the peak demand 5.3 MW, and we only optimize over $(\gamma_1,\gamma_2,\bar{b})$.

The capital cost, the operation/maintenance cost, and the lifetime of each system component are given in Table II.

2) An optimal design $(\gamma_1^*,\gamma_2^*,\bar{b}^*)$: We now present an example design by solving the optimization problems (11)–(12) and (13)–(14). We will use $\epsilon = 10\%$ as the acceptable risk (recall that the load-shedding event in our model will likely correspond to the need to invoke diesel or gas backup generation in practice). For simplicity of illustration, we respectively fix the battery capacity as $\bar{b} = 15$ MWh and $\bar{b} = 20$ MWh and focus on sizing the PV arrays and wind turbines.

Figure 10 shows the variation of the total construction and operation cost as a function of γ_1 and γ_2 with battery capacity of $\bar{b} = 15$ MWh. The numbers on the curves are the total cost in dollars. There are at least two points that are of interest.

TABLE II
COST MODEL PARAMETERS FOR CATALINA CASE STUDY.

Name	*Cost Data*	*Sources*
Life	20 years	
PV Array		
C_{module}	2.80 \$/W	[10] for utility-scale PV
$C_{O\&M1}$	15 \$/kW-yr	[11]
Wind Turbine		
$C_{turbine}$	2,300 \$/per turbine	[12] for 1 kW turbine
$C_{O\&M2}$	20 \$/kW-yr	[10]
Battery		
$C_{battery}$	211 \$/kWh	[13]
Converter		
$C_{converter}$	0.715 \$/W	[13]

- As renewable generation size increases, C increases linearly.
- If we look for an optimal solution $(\gamma_1^*,\gamma_2^*,\bar{b}^*)$ under certain constraint, e.g, $F_t \leq 10\%$, we need to find the left-most intersection of two curves $F_t = 10\%$ and C. By this approach, the combination $(\gamma_1^*,\gamma_2^*,\bar{b}^*)$ at this intersection is the optimal solution becasue C is the least and F_t belongs to the specified risk level. On the other hand, if constraint is $F_e \leq 10\%$, we need to find the left-most intersection of two curves $F_e = 10\%$ and C.

The variation of the total construction and operation cost as a function of γ_1 and γ_2 with battery capacity of $\bar{b} = 20$ MWh is almost the same as Figure 10. The only difference is that for fixed γ_1 and γ_2, C is less with $\bar{b} = 15$ MWh than that with $\bar{b} = 20$ MWh, since $\bar{b}$ is larger and costs more here. We will not present the figure with $\bar{b} = 20$ MWh again due to the similarity.

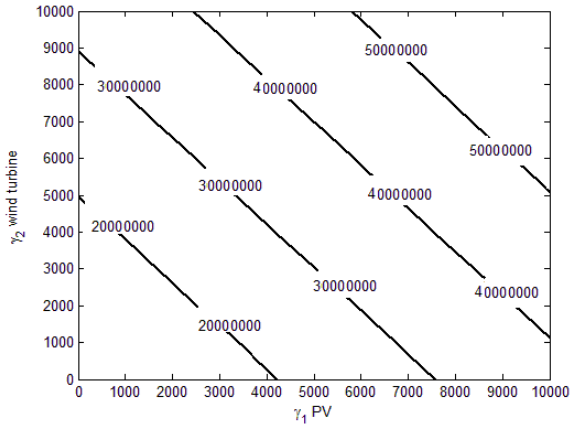

Fig. 10. The variation trend of the total construction and operation cost with battery capacity of $\bar{b} = 15$ MWh.

Figure 11 shows the optimal design in problems (11)–(12) with $\bar{b} = 15$ MWh. Here we set the constraint of $F_t \leq 10\%$. The optimal point in Figure 11 is the combination of 4300 kW PV arrays and 4000 wind turbines, with C=\$30,352,402. Figure 12 shows the optimal design in problems (13)–(14) with $\bar{b} = 15$ MWh. Here we set the constraint of $F_e \leq 10\%$. The optimal point in Figure 12 is the combination of 3650 kW PV arrays and 3000 wind turbines, with C=\$25,891,174. More

detailed results are shown in Table III, giving us the optimal size of PV arrays, number of wind turbines and battery capacity that minimizes the total construction and operation cost in the same acceptable risk level. In this table, COE means cost of energy. Note that battery capacity has a large effect both on F_t or F_e and C. For fixed F_t or F_e, C and COE is much less with $\bar{b} = 20$ MWh than that with $\bar{b} = 15$ MWh. In addition, the estimated renewable cost is comparable since the conventional power cost in U.S. is 9.48 cent/kWh in 2009 [14].

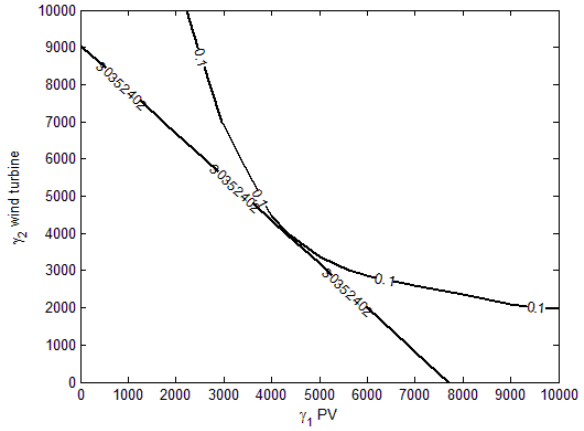

Fig. 11. The optimal solution to the problem: minimize total cost subject to $F_t \leq 0.1$ with $\bar{b} = 15$ MWh.

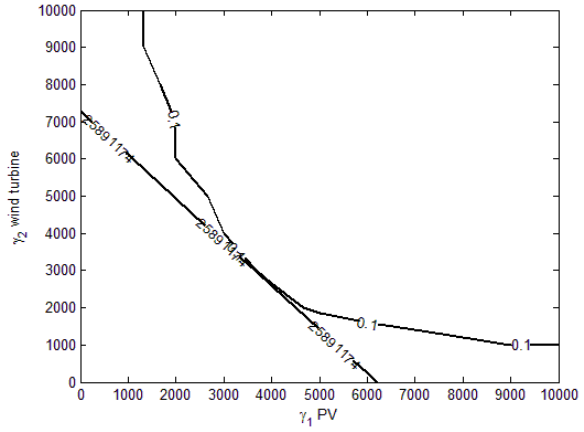

Fig. 12. The optimal solution to the problem: minimize total cost subject to $F_e \leq 0.1$ with $\bar{b} = 15$ MWh.

V. Conclusion

The objective of the study is investigating the feasibility of replacing diesel generation with renewable generation supplemented with battery storage for a case study. We formulated optimal design problems in order to illustrate the tradeoff between the total construction and operation cost and acceptable risk levels.

We presented our simulation results from HOMER simulator and calculated some cost estimations of an off-grid hybrid energy system with PV/ wind turbine/ storage for the case study representing key characteristics of the setting on Catalina Island, assuming the weather resources and load keeps unchanged.

Limited in this study, but future research will include considering the effects of stochastic weather, load profiles, transimission and distribution of the power network on Catalina on the design results and make comparison with the results of [8]. We will also leave the viability analysis to our future work with SCE.

TABLE III
SUMMARY OF THE OPTIMAL RESULTS.

PV Arrays	Wind Turbine	Battery Capacity (MWh)	F_t	C ($)	COE ($/kWh)
4,300	4,000	15	10%	30,352,402	0.201
PV Arrays	Wind Turbine	Battery Capacity (MWh)	F_t	C ($)	COE ($/kWh)
3,930	3,000	20	10%	27,778,348	0.185
PV Arrays	Wind Turbine	Battery Capacity (MWh)	F_t	C ($)	COE ($/kWh)
3,650	3,000	15	10%	25,891,174	0.177
PV Arrays	Wind Turbine	Battery Capacity (MWh)	F_t	C ($)	COE ($/kWh)
3,000	3,000	20	10%	25,014,342	0.172

References

[1] Ajai Gupta, R. P. Saini and M. P. Sharma, Hybrid Energy System for Remote Area - An Action Plan for Cost Effective Power Generation, Industrial and Information Systems, IEEE Region 10 and the Third international Conference, December 8-10, 2008.

[2] K. Kurokawa, K. Kato, M. Ito, K. Komoto, T. Kichimi and H. Sugihara, A Cost Analysis of Very Large Scale System on the World Deserts, Photovoltaic Specialists Conference, Conference Record of the Twenty-Ninth IEEE, pp. 1672-1675, 2002.

[3] P. D. Klemper, M. A. Meyer, W. D. Kellogg, M.H. Nehriri, G. Venkataramanan and V. Gerez, Generation Unit Sizing And Cost Analysis for Stand-alone Wind, PV And Hybrid Wind/PV Systems, IEEE Transactions on Energy Conversion, Vol. 13, No. 1, pp. 70-75, March, 1998.

[4] P. P. Varaiya, F. F. Wu and J. W. Bialek, Smart operation of smart grid: risk-limiting dispatch, Proc. of IEEE, 99(1): 40–57, January, 2011.

[5] http://www.homerenergy.com/.

[6] http://rredc.nrel.gov/solar/olddata/nsrdb/

[7] http://wind.nrel.gov/webnrel/

[8] Huan Xu, Ufuk Topcu, S. Low, C. R. Clarke and K.M. Chandy, Load-shedding probabilities with hybrid renewable power generation and energy storage, Communication, Control and Computing, 48th, Annual Allerton Conference, pp. 233, 2010.

[9] A. Rohani, K. Mazlumi and H. Kord, Modeling of a Hybrid Power System for Economic Analysis and Environmental Impact in HOMER, Electrical Engineering (ICEE), 18th Iranian Conference, pp. 819-823, May 11-13, 2010.

[10] Aabakken, J, Power Technologies Energy Data Book, fourth edition. National Renewable Energy Laboratory (NREL), Golden, CO, 2006.

[11] C. P. Cameron and A. C. Goodrich, The Levelized Cost of Energy for Distributed PV: A Parametric Study, Photovoltaic Specialists Conference (PVSC), 35th IEEE, pp. 529 - 534, 2010.

[12] P. Kwartin, A. Wolfrum, K. Granfield and A. Kagel, An Analysis of the Technical and Economic Potential for Mid-Scale Distributed Wind, Subcontract Report NREL/SR-500-44280, December, 2007- October 31, 2008.

[13] http://www.solarbuzz.com/

[14] http://www.skepticalscience.com/true-cost-of-coal-power.html/